Materials Transactions, Vol. 42, No. 7 (2001) pp. 1182 to 1189
Special Issue on Platform Science and Technology for Advanced Magnesium Alloys

The Grain Size and Texture Dependence of Tensile Properties in Extruded Mg–9Al–1Zn

Mamoru Mabuchi[1], Yasumasa Chino[1], Hajime Iwasaki[2], Tatsuhiko Aizawa[3] and Kenji Higashi[4]

[1]*National Institute of Advanced Industrial Science and Technology, Nagoya 462-8510, Japan*
[2]*College of Engineering, Department of Materials Science and Engineering, Himeji Institute of Technology, Himeji 671-2201, Japan*
[3]*Research Center for Advanced Science and Technology, The University of Tokyo, Tokyo 153-8904, Japan*
[4]*College of Engineering, Department of Metallurgy and Materials Science, Osaka Prefecture University, Sakai 599-8531, Japan*

The tensile properties at room temperature ~ 573 K of Mg–9Al–1Zn processed by normal extrusion were compared with those processed by equal channel angular (ECA) extrusion. The strength at room temperature was strongly affected by the grain size. However, the effect of the grain size rapidly decreased with testing temperature. At room temperature, the normal extruded alloy showed the stronger grain size dependence of 0.2% proof stress than the ECA extruded alloy because of the microscopic orientation effect. Also, the grain size dependence was reduced when grain boundaries were in a non-equilibrium state.

(Received January 16, 2001; Accepted April 9, 2001)

Keywords: *magnesium alloy, extrusion, mechanical properties, grain size dependence, non-equilibrium grain boundary*

1. Introduction

Magnesium alloys are promising structural light metals because of their low densities, good recycling potential and abundant resources. To date, most of Mg products have been fabricated through casting routes.[1,2] On the other hand, there are few applications of plastic forming process in Mg products.[3] To increase applications of Mg alloys, it is important to develop a plastic forming process technology for Mg alloys.

Recently, it has been reported[4] that the mechanical properties of Mg alloys can be significantly improved by grain refinement, for example, a powder metallurgy Mg–Al–Zn alloy with a small grain size of 0.5 μm showed high strength of 432 MPa[5] and superplasticity at a high strain rate of 10^{-2} s^{-1}.[6] In general, the tensile flow stress at room temperature depends on the grain size, according to the Hall-Petch relation[7,8]

$$\sigma = \sigma_0 + Kd^{-1/2} \quad (1)$$

where σ is the tensile flow stress of a polycrystalline metal, σ_0 is the tensile flow stress if there is no resistance to slip across grain boundaries, K is a constant and d is the grain size. The hcp metals such as Mg exhibit a large value of K, namely, the strong grain size dependence of flow stress, compared to bcc and fcc metals.[9,10] Furthermore, texture strongly affects the mechanical properties in hcp metals.[11] Both grain refinement due to recrystallization and high intensity of texture can be attained through hot or warm working. Therefore, it is important to investigate the mechanical properties of hot- or warm-worked Mg alloys from the viewpoint of the texture and grain size dependence of flow stress.

Fine-grained microstructure has been attained in a Mg–9Al–1Zn alloy by normal extrusion[12] and equal channel angular (ECA) extrusion.[13] For these processes, texture formed by normal extrusion is considered to be different from that formed by ECA extrusion. However, there have been no studies describing differences in mechanical properties between normal extruded Mg alloys and ECA extruded Mg alloys. In the present paper, the mechanical properties of Mg–9Al–1Zn processed by normal extrusion are compared with those processed by ECA extrusion in a grain size range of 0.5–60 μm and in a temperature range of room temperature ~ 573 K from the viewpoint of the texture and grain size dependence of flow stress.

2. Experimental Procedure

A Mg alloy used in the present investigation was a Mg–9 mass%Al–0.8 mass%Zn–0.3 mass%Mn alloy. Bars of 40 mm dia. were machined from a cast ingot and then normal extrusion was carried out at 473, 523, 623 and 723 K with a reduction ratio of 4.9 : 1. Bars of 20 mm dia. were also machined from the cast ingot and then ECA extrusion was carried out at 448, 458, 523, 623 and 673 K with a total strain[14] of 6.342. The number of repetitive ECA extrusion was 6 and the bars were not rotated between each extrusion. The angle of intersection between the two channels was 90°. The specimen processed by ECA extrusion at 448 K was the same as that in the previous work,[13] which revealed that grain boundaries in the specimen processed by ECA extrusion at 448 K were in a non-equilibrium state, namely, the crystal lattice near the grain boundaries was highly distorted.[13] On the other hand, except the one processed by ECA extrusion at 448 K, the distortion of the lattice plane was not observed near the grain boundaries and grain boundaries were in an equilibrium state.

Tensile specimens with a gage length of 10 mm and a gage diameter of 2.5 mm were machined from the central region of as-extruded rods. Tensile tests were carried out at room temperature ~ 573 K and at an initial strain rate of 1.7×10^{-3} s^{-1} in air. The tensile axis was selected to be parallel to the extrusion direction. For the tensile tests at elevated temperatures, the specimens required 1.8×10^3 s to equilibrate at the test

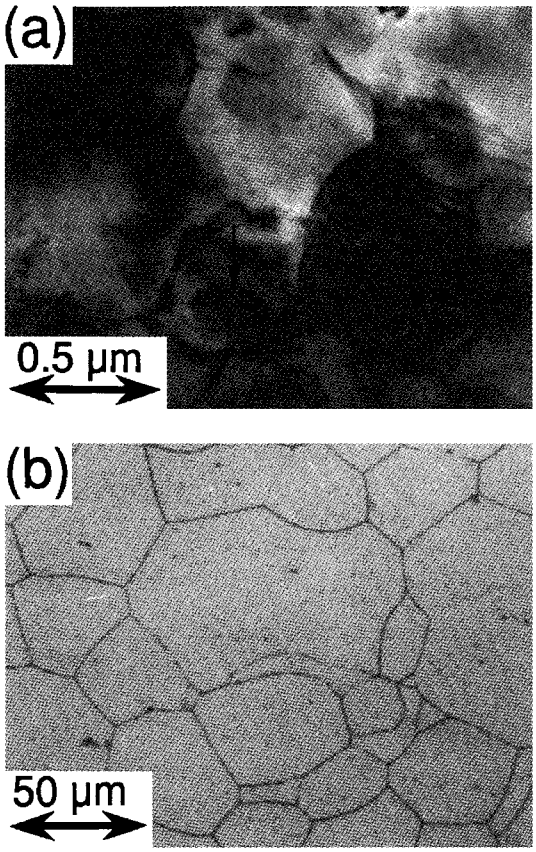

Fig. 1 Microstructures of the normal extruded Mg–9Al–1Zn, (a) the extrusion at 473 K and (b) the extrusion at 723 K.

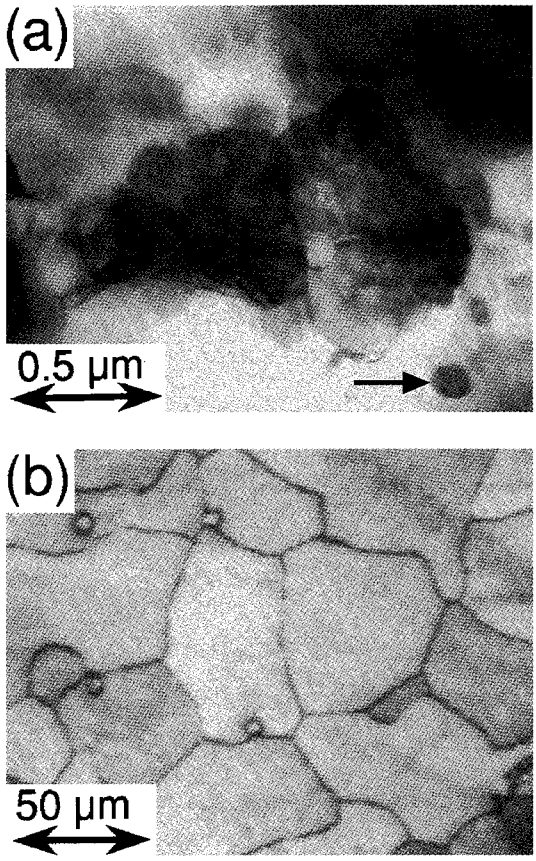

Fig. 2 Microstructures of the ECA extruded Mg–9Al–1Zn, (a) the extrusion at 458 K and (b) the extrusion at 673 K.

temperature prior to straining. The temperature variation during tensile tests was less than ±1 K. Microstructure was investigated by an optical microscope and a transmission electron microscope. Fracture surface was observed by a scanning electron microscope. The (0001) pole figures were examined using the longitudinal cross section. Also, the distribution of grain boundary misorientations was investigated by an electron backscattered diffraction method.[15]

3. Results

3.1 Microstructure

Microstructures of the normal extruded alloy and the ECA extruded alloy are shown in Fig. 1 and Fig. 2, respectively. The grains were equiaxed for both the normal extruded alloy and the ECA extruded alloy. An arrow in (a) shows a precipitate. On the other hand, precipitates are not observed in (b). Thus, precipitation states of the precipitate size and interspacing in the normal extruded alloy and the ECA extruded alloy were almost the same when the normal extrusion temperature was the same as or close to the ECA extrusion temperature.

The grain sizes of the normal extruded and the ECA extruded alloys are listed in Table 1. The grain size significantly decreased with decreasing extrusion temperature for both the normal extruded alloy and the ECA extruded alloy. A small grain size of 1.2 μm was attained by normal extrusion at 473 K and a small grain size of 0.5 μm was attained by ECA extrusion at 448 K.

The (0001) pole figures of the specimens processed by normal extrusion at 523 K and by ECA extrusion at 523 K are shown in Fig. 3. In the normal extruded alloy, the basal slip planes were almost parallel to the extrusion direction, as shown in Fig. 3(a). This trend is the same as the result by Wilson and Chapman.[16] On the other hand, the (0001) pole figure of the ECA extruded alloy showed that the basal slip planes were not parallel to the extrusion direction. Clearly, the texture of the ECA extruded alloy was different from that of the normal extruded alloy. The similar difference in texture between the normal extruded alloy and the ECA extruded alloy was observed in all the specimens.

Table 1 The grain size of the normal extruded and the ECA extruded Mg–9Al–1Zn alloys.

	Extrusion temperature (K)	Grain size (μm)
Normal extrusion	473	1.2
	523	2.1
	623	15.6
	723	59.1
ECA extrusion	448	0.5*
	458	1.0
	523	2.0
	623	12.6
	673	60.9

*Non-equilibrium grain boundaries (Ref. 13))

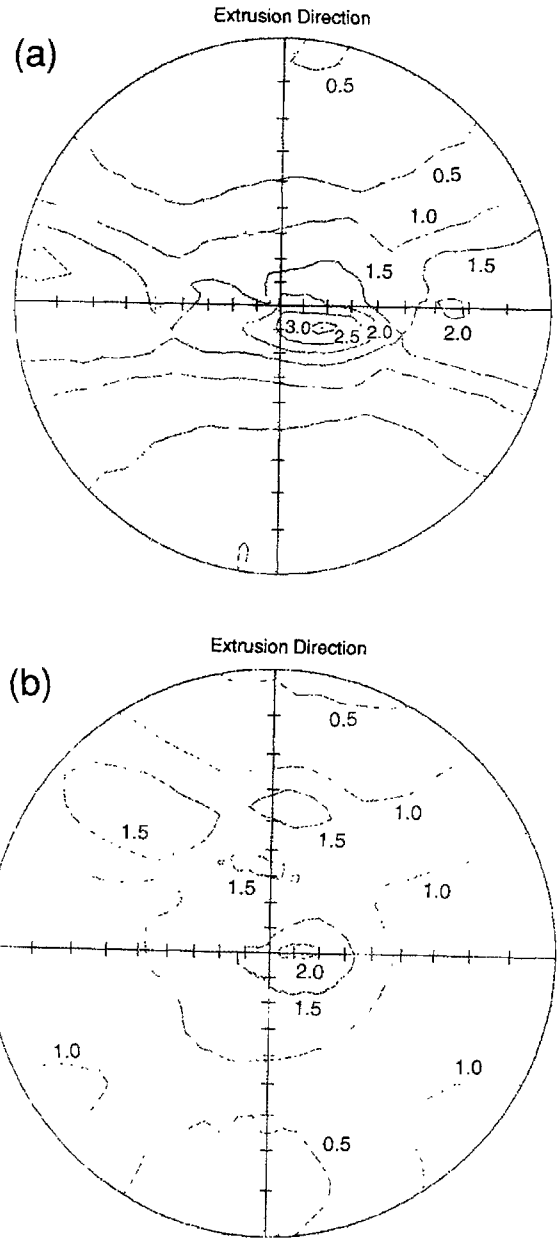

Fig. 3 (0001) pole figures of the normal extruded alloy and the ECA extruded alloy, (a) the normal extrusion at 523 K and (b) the ECA extrusion at 523 K.

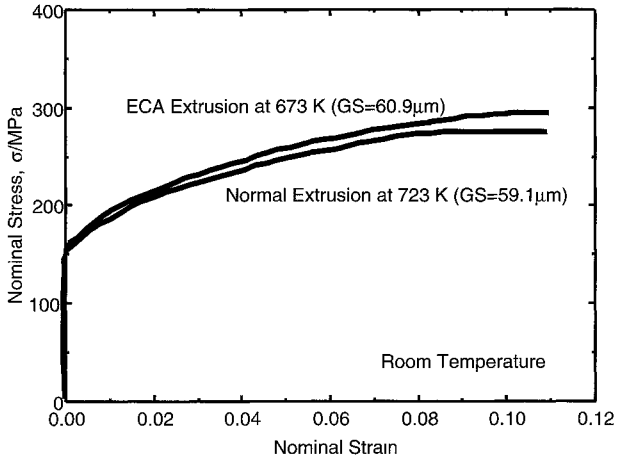

Fig. 4 The nominal stress-nominal strain curves at room temperature of the normal extruded alloy at 723 K and the ECA extruded alloy at 673 K. The grain sizes of the normal extruded alloy at 723 K and the ECA extruded alloy at 673 K are almost the same (= about 60 μm).

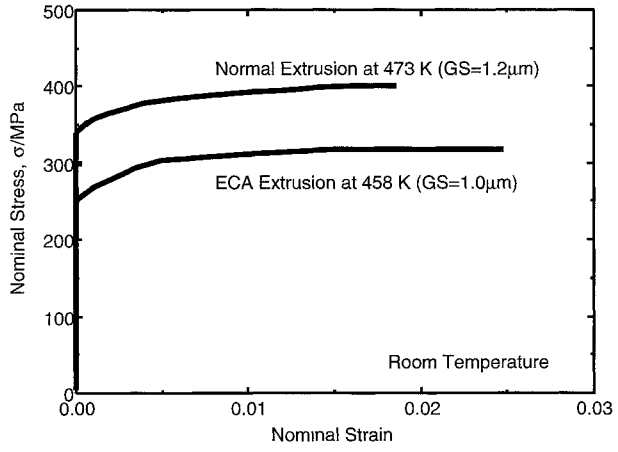

Fig. 5 The nominal stress-nominal strain curves at room temperature of the normal extruded alloy at 473 K and the ECA extruded alloy at 458 K. The grain sizes of the normal extruded alloy at 473 K and the ECA extruded alloy at 458 K are almost the same (= about 1 μm).

3.2 Tensile properties

The nominal stress-nominal strain curves at room temperature of the normal extruded alloy at 723 K and the ECA extruded alloy at 673 K are shown in Fig. 4. The grain sizes of the normal extruded alloy at 723 K and the ECA extruded alloy at 673 K are almost the same (= about 60 μm). It can been seen that there is little difference in flow stress between the normal extruded alloy at 723 K and the ECA extruded alloy at 673 K.

The nominal stress-nominal strain curves at room temperature of the normal extruded alloy at 473 K and the ECA extruded alloy at 458 K are shown in Fig. 5. Both the normal extruded alloy at 473 K and the ECA extruded alloy at 458 K showed a very small grain size of about 1 μm. Also, precipitation states of the precipitate size and interspacing between both the specimens were almost the same. It should be noted that the flow stress of the normal extruded alloy at 473 K was higher than that of the ECA extruded alloy at 458 K, in spite of the same grain size.

The results of tensile tests at room temperature in the normal extruded and ECA extruded alloys are summarized in Table 2. When the normal extruded alloy and the ECA extruded alloy with the same grain size are compared, the former shows higher 0.2% proof stress and higher ultimate tensile strength than the latter in case of the grain size $\leq$ about 16 μm, however, there is little difference in 0.2% proof stress and ultimate tensile strength between the former and the latter in case of the grain size=about 60 μm.

It is well known that twin deformation often occurs in Mg and its alloys.[17] Lahaie *et al.*[18] noted that twin deformation occurs more easily in a Mg alloy with a large grain size than in a Mg alloy with a small grain size. In the present investigation, twin was observed near the fracture surface in all the specimens deformed to failure at room temperature for both the normal extruded and the ECA extruded alloys. However, no evidence for twin deformation was observed in the specimens deformed to $\varepsilon = 0.2\%$ for both the normal extruded

Table 2 Tensile properties at room temperature in the normal extruded and the ECA extruded Mg–9Al–1Zn alloys.

	Extrusion temperature (K)	0.2% Proof stress (MPa)	Tensile strength (MPa)	Elongation failure (%)
Normal extrusion	473	364	400	1.9
	523	278	302	1.4
	623	227	325	7.1
	723	158	274	11.0
ECA extrusion	448*	273	313	3.2
	458	277	318	2.5
	523	231	298	5.2
	623	182	320	12.4
	673	164	293	11.0

* Non-equilibrium grain boundaries (Ref. 13))

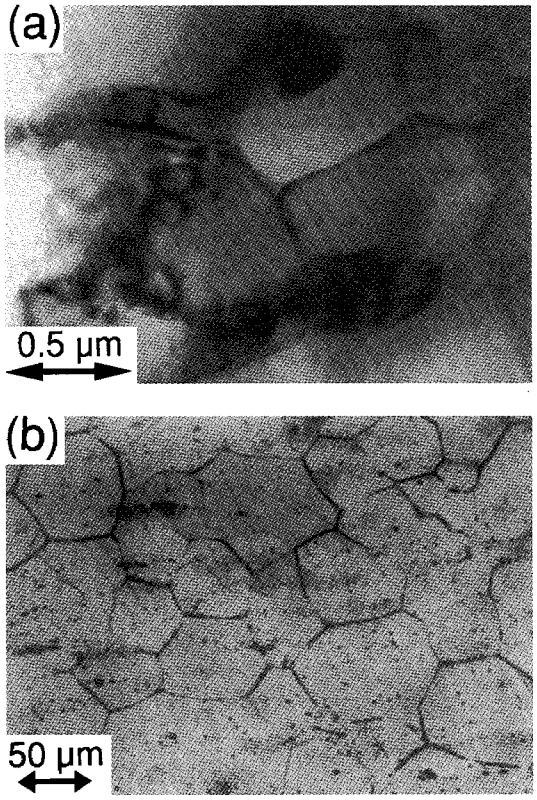

Fig. 6 Microstructures of the normal extruded alloy deformed to $\varepsilon = 0.2\%$ at room temperature, showing no evidence for twin deformation, (a) the extrusion at 473 K and (b) the extrusion at 723 K.

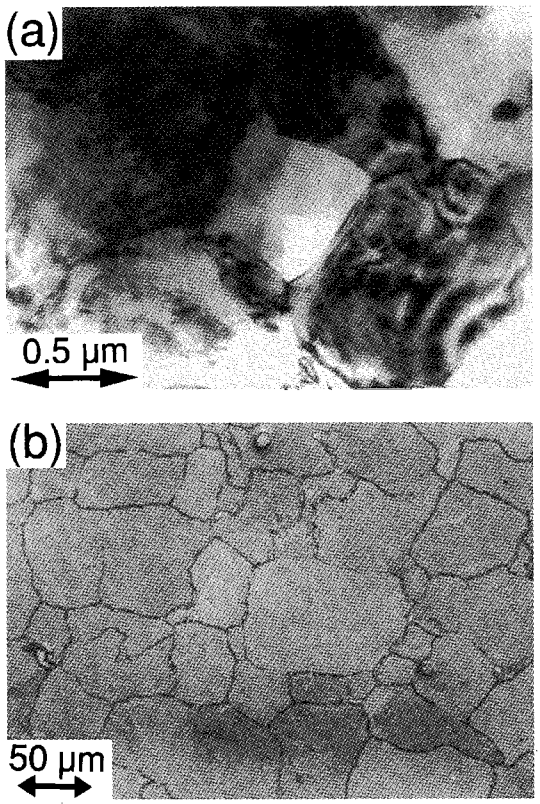

Fig. 7 Microstructures of the ECA extruded alloy deformed to $\varepsilon = 0.2\%$ at room temperature, showing no evidence for twin deformation, (a) the extrusion at 458 K and (b) the extrusion at 673 K.

and the ECA extruded alloys, as shown in Fig. 6 and Fig. 7. Therefore, it is suggested that the grain size dependence of 0.2% proof stress is not associated with twin deformation.

Another important result in Table 2 is that the elongation to failure tends to decrease with decreasing grain size for both the normal extruded alloy and the ECA extruded alloy. This trend is the same as that of aluminum alloys.[19] However, Chapman and Wilson[20] showed that the elongation to failure of Mg increased with decreasing grain size. Mohri *et al.*[21] noted that the fracture mode changed from intergranular fracture to transgranular fracture by grain refinement, resulting in an increase in elongation to failure with decreasing grain size. Such drastic change in fracture mode was not observed in the present investigation. Therefore, it is suggested that the elongation to failure decreases with decreasing grain size in Mg as well as other metals when the fracture mechanism does not change. Also, cleavage fracture was partially observed in the specimens with a small grain size of less than 2 μm for both the normal extruded alloy and the ECA extruded alloy (Fig. 8). The cleavage fracture may be related to the low elongation in the alloys with a small grain size.

It is of interest to note that the ECA extruded alloy at 448 K, whose grain boundaries were in a non-equilibrium state,[13] showed the same strength as the ECA extruded alloy at 458 K though the grain size of the former was smaller than that of the latter. This fact shows that resistance to slip across the grain boundaries is reduced due to a non-equilibrium state of grain boundaries, suggesting that the high distortion of crys-

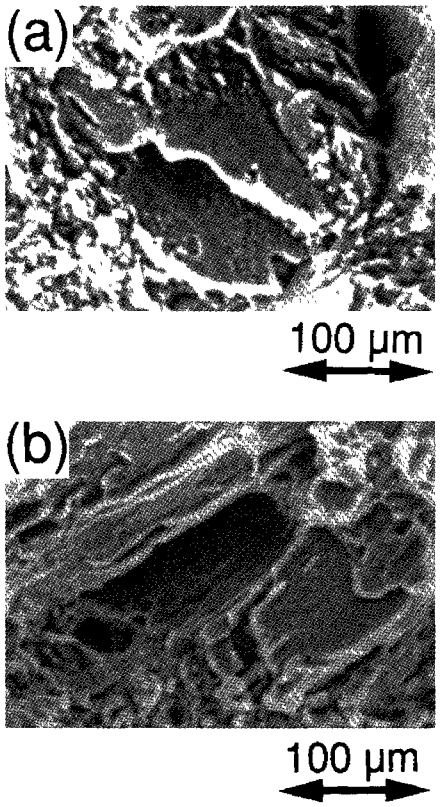

Fig. 8 Cleavage fracture observed on the fracture surface, (a) the normal extruded alloy at 473 K and (b) the ECA extruded alloy at 448 K.

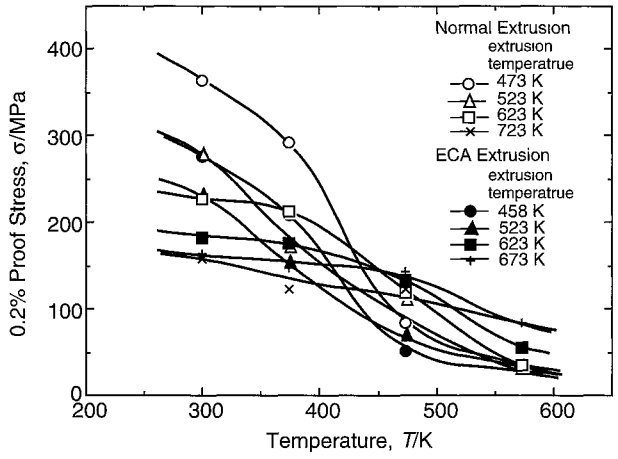

Fig. 9 The variation in 0.2% proof stress as a function of testing temperature.

tal lattice near the grain boundaries affects the operation of a dislocation source.

The variation in 0.2% proof stress as a function of testing temperature is shown in Fig. 9, the variation in ultimate tensile strength as a function of testing temperature is shown in Fig. 10, and the variation in elongation to failure as a function of testing temperature is shown in Fig. 11, respectively. It can be seen that the 0.2% proof stress is strongly affected by the grain size at room temperature, however, the effect of the grain size tends to be reduced rapidly with increasing temperature. On the other hand, the elongation to failure depended on the grain size at elevated temperatures as well as room temperature.

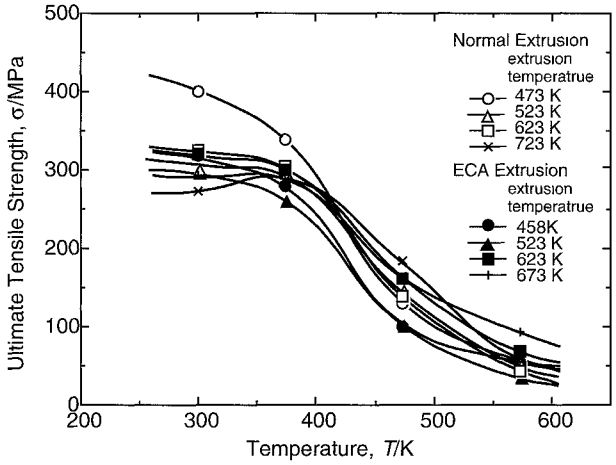

Fig. 10 The variation in ultimate tensile strength as a function of testing temperature.

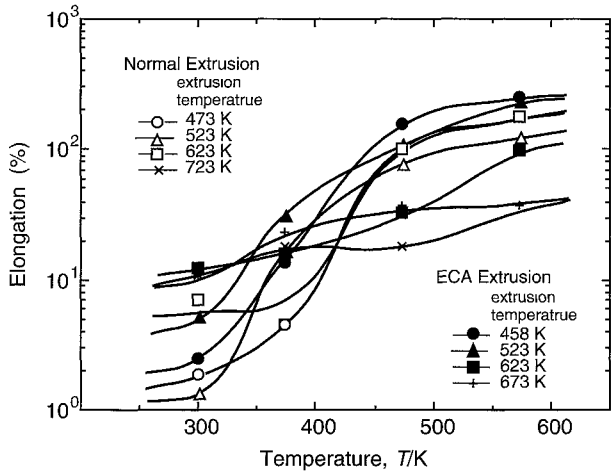

Fig. 11 The variation in elongation to failure as a function of testing temperature.

4. Discussion

The flow stress of Mg strongly depends on the grain size.[9,10] The strong grain size dependence of flow stress in Mg is because Mg has the large orientation factors which arise from the lack of slip systems.[9] Another unique character of Mg is the strong texture dependence which is attributed to large difference in critical shear stress between the basal plane and the non-basal planes. Both the lack of slip systems and the large difference in critical shear stress between the basal plane and the non-basal planes are the intrinsic characteristics of hcp metals, which are attributed to anisotropy of atomic bonding. Hence, the origins of the strong grain size dependence and the strong texture dependence of flow stress are the same. It is well known that the difference in critical shear stress between the basal plane and the non-basal planes decreases with increasing temperature.[22,23] It is therefore suggested that not only the effect of texture, but also the effect of grain size on the flow stress are reduced with temperature. This is consistent with the fact that the effect of the grain size on the 0.2% proof stress rapidly decreased with increasing testing temperature, as shown in Fig. 9.

At room temperature, the relationship between the grain

size dependence of flow stress and the texture can be discussed using the Hall-Petch relation. The 0.2% proof stress of the normal extruded alloy and the ECA extruded alloy can be represented as a function of (grain size)$^{-1/2}$ according to the Hall-Petch relation when the effect of precipitation on the 0.2% proof stress is small. The results are shown in Fig. 12. The data of each alloy can be reasonably fitted to a line. A value of the tensile flow stress in case of no resistance to slip across grain boundaries, σ_0, of the normal extruded alloy was not largely different from that of the ECA extruded alloy. However, the slope of a line, namely, the grain size dependence of K, of the normal extruded alloy was much larger than that of the ECA extruded alloy.

From the relation of $\sigma = m\tau$ (σ: tensile stress and τ: shear stress), σ_0 is given by

$$\sigma_0 = m\tau_{\mathrm{CRSS}} \tag{2}$$

where m is the Taylor orientation factor and τ_{CRSS} is the single crystal critical resolved shear stress. The Taylor orientation factor, m, is the macroscopic orientation factor. Armstrong *et al.*[9] pointed out the importance of a local orientation problem in operating a dislocation source ahead of a blocked slip band. Taking into consideration a local orientation problem, a constant in the Hall-Petch equation, K, can be given by[24]

$$K = cm\{m^*Gb\tau_c/(1-\nu)\}^{1/2} \tag{3}$$

where m^* is the Sachs orientation factor, G is the shear modulus, b is the dislocation Burgers vector, τ_c is the shear stress required to operate a dislocation source in the slip plane of the source, ν is the Poissons ratio and c is a constant. The Sachs orientation factor relating the applied stress to the average shear stress on a particular slip system-type, m^*, is the microscopic orientation factor. The result in Fig. 12 revealed that a value of σ_0 of the normal extruded alloy was not largely different from that of the ECA extruded alloy, however, a value of K of the former was much larger than that of the latter. This indicates that the difference in grain size dependence of 0.2% proof stress is attributed to the microscopic orientation effect, not to the macroscopic orientation effect. Wilson and Chapman[16] investigated the effect of preferred orientation on the grain size dependence of yield stress of Mg and they also pointed out the importance of the microscopic orientation effect. Texture is considered to affect both the macroscopic and microscopic orientation factors. It is therefore suggested that at least under conditions investigated in the present paper, texture strongly affects the microscopic orientation, not the macroscopic orientation. As listed in Table 2, the normal extruded alloy at 473 K showed high 0.2% proof stress of 364 MPa and high strength of 400 MPa. The high strength of the normal extruded alloy is attributed not only to a small grain size of 1 μm, but also to the microscopic orientation effect.

It is well known that misorientations of grain boundaries affect the grain size dependence of flow stress, for example, a value of K for low angle boundaries is about half of that for high angle boundaries.[25] Distribution of misorientations of grain boundaries is shown in Fig. 13 for the specimen processed by normal extrusion at 723 K and in Fig. 14 for the specimen processed by ECA extrusion at 673 K, respectively. The frequency of low angle boundaries is larger for the ECA extrusion than for the normal extrusion. However, the difference in frequency of low angle boundaries between the normal extrusion and the ECA extrusion is too small to explain the large difference in grain size dependence of 0.2% proof stress. It is of interest to note that there are three peaks in Fig. 14 and the distribution of grain boundary misorientations is unusual in the ECA extrusion. Therefore, the distribution of grain boundary misorientations may affect the microscopic orientation effect. It is accepted[26–28] that there are special grain boundaries such as coincidence grain boundaries whose characteristics are different from those of high angle boundaries. Watanabe *et al.*[28] investigated the effect of misorientations on sliding in Zn and they revealed that the sliding rate rapidly decreased at a special misorientation. The large frequency of special grain boundaries such as coincidence grain boundaries may affect the microscopic orientation effect. However, the coincidence grain boundaries in hcp metals were too complicated to determine by an electron backscattered diffraction method in the present investigation. Further research is needed to understand effects of the microscopic orientation factor on the grain boundary dependence of flow stress.

Another important result in Fig. 12 is that the 0.2% proof

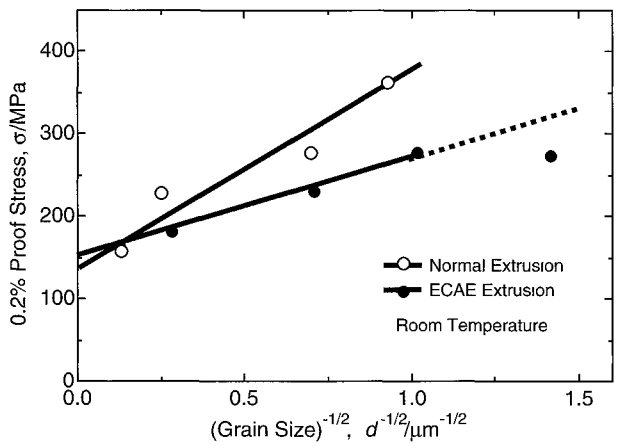

Fig. 12 The variation in 0.2% proof stress at room temperature as a function of (grain size)$^{-1/2}$.

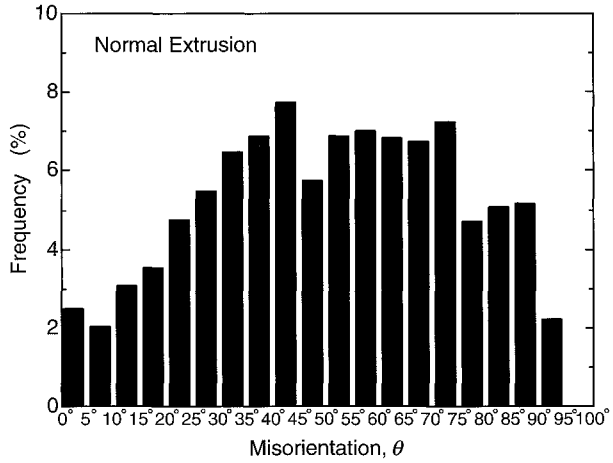

Fig. 13 Distribution of grain boundary misorientations of the specimen processed by normal extrusion at 723 K.

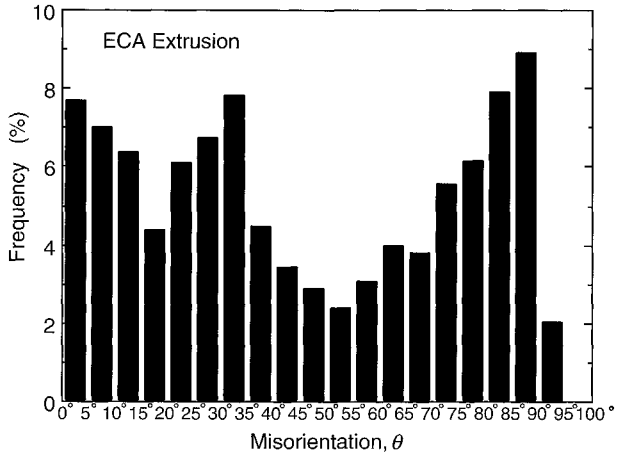

Fig. 14 Distribution of grain boundary misorientations of the specimen processed by ECA extrusion at 673 K.

stress of the ECA extruded alloy with the smallest grain size of 0.5 μm, whose grain boundaries are in a non-equilibrium state,[13] is much lower than a value expected from the line fitted by the other data. The same trend have been reported in Al alloys[29,30] and a Mg alloy.[31] Wyrzykowski and Grabski[32] showed that the grain boundary structure affects the grain size dependence of flow stress in pure Al. Valiev *et al.*[29] suggested that non-equilibrium grain boundaries may be more transparent for mobile dislocations. Also, Furukawa *et al.*[30] noted that the small grain size dependence of stress in an Al alloy with non-equilibrium grain boundaries is because of the increased participation of mobile extrinsic dislocations in the grain boundary regions. The grain size dependence of flow stress is determined by the orientation factors, the shear modulus and the shear stress required to operate a dislocation source in the slip plane of the source. The orientation factors and the shear modulus of the ECA extruded specimen with a grain size of 0.5 μm are considered to be the same as those of the other ECA extruded specimens. Hence, the low 0.2% proof stress of the ECA extruded alloy with a grain size of 0.5 μm is probably because the shear stress required to operate a dislocation source is reduced due to the non-equilibrium grain boundaries. A lot of dislocations were piled up in a narrow range of 10 nm from the grain boundary in the ECA extruded alloy with a grain size of 0.5 μm.[13] Valiev *et al.*[33] and Nazarov *et al.*[34] analyzed the stress fields caused by non-equilibrium grain boundaries and they noted that non-equilibrium grain boundaries have long-range stress fields near the grain boundaries. Therefore, it is probable that the stress fields make unlocking of dislocation easy, resulting in reduction of the shear stress required to operate a dislocation source.

5. Conclusions

(1) In the present paper, the mechanical properties of Mg–9Al–1Zn processed by normal extrusion were compared with those processed by ECA extrusion in a grain size range of 0.5–60 μm and in a temperature range of room temperature ~ 573 K.

(2) At room temperature, there was large difference in 0.2% proof stress between the normal extruded alloy and the ECA extruded alloy in case of a small grain size of less than about 16 μm, however, little difference in case of a large grain size of about 60 μm.

(3) The elongation to failure decreased with decreasing grain size for both the normal extruded alloy and the ECA extruded alloy.

(4) The normal extruded alloy showed the stronger grain size dependence of 0.2% proof stress at room temperature than the ECA extruded alloy because of difference in microscopic orientation factor, which is likely to be related to the distribution of grain boundary misorientations.

(5) The ECA extruded alloy at 448 K, whose grain boundaries were in a non-equilibrium state, showed the same strength as the ECA extruded alloy at 458 K, in spite of the smaller grain size. It is suggested that the shear stress required to operate a dislocation source decreases due to the stress fields caused by non-equilibrium grain boundaries.

Acknowledgments

The authors are grateful to Dr. N. Saito and Mr. H. Ichiryu for electron backscattered diffraction observation and tensile tests. M. M. gratefully acknowledges the financial support from the project "Barrier-Free Processing of Materials for Life-Cycle Design for Environment" by Science and Technology Agency. Also, M. M., T. A. and K. H. gratefully acknowledge the financial support from the Ministry of Education, Science, Culture and Sports, Japan as the Priority Area "Platform Science and Technology for Advanced Magnesium Alloys".

REFERENCES

1) D. Magers and J. Willekens: *Magnesium Alloys and Their Applications*, ed. by B. L. Mordike and K. U. Kainer, (Werkstoff-Informationsgesellschaft mbH, Frankfurt, 1998) pp. 105–108.
2) R. Decker, R. Carnahan, R.Vining, D. Walukas, S. LeBeau and N. Prewitt: *Magnesium Alloys and Their Applications*, ed. by B.L.Mordike and K.U.Kainer, (Werkstoff-Informationsgesellschaft mbH, Frankfurt, 1998) pp. 545–550.
3) J. Becker, G. Fischer and K. Schemme: *Magnesium Alloys and Their Applications*, ed. by B. L. Mordike and K. U. Kainer, (Werkstoff-Informationsgesellschaft mbH, Frankfurt, 1998) pp. 15–28.
4) K. Kubota, M. Mabuchi and K. Higashi: J. Mater. Sci. **34** (1999) 2255–2262.
5) H. Iwasaki, K. Yanase, T. Mori, M. Mabuchi and K. Higashi: J. Jpn Soc. Powder and Powder Metall. **43** (1996) 1350–1353.
6) M. Mabuchi, T. Asahina, H. Iwasaki and K. Higashi: Mater. Sci. Tech. **13** (1997) 825–831.
7) E. O. Hall: Proc. Phy. Soc., Lond. **B 64** (1951) 747.
8) N. J. Petch: J. Iron Steel. Inst. **174** (1953) 25.
9) R. Armstrong, I. Codd, R. M. Douthwaite and N. J. Petch: Philos. Mag. **7** (1962) 45–58.
10) M. Mabuchi and K. Higashi: Acta Mater. **44** (1996) 4611–4618.
11) S. E. Ion, F. J. Humphreys and S. H. White: Acta Metall. **30** (1982) 1909–1919.
12) M. Mabuchi, K. Kubota and K. Higashi: Mater. Trans., JIM **36** (1995) 1249-1254.
13) M. Mabuchi, K. Ameyama, H. Iwasaki and K. Higashi: Acta Mater. **47** (1999) 2047–2057.
14) Y. Iwahashi, J. Wang, Z. Horita, M. Nemoto and T. G. Langdon: Scr. Mater. **35** (1996) 143–146.
15) D. J. Dingley and D. P. Field: Mater. Sci. Tech. **13** (1997) 69–78.
16) D. V. Wilson and J. A. Chapman: Philos. Mag. **8** (1963) 1543–1551.
17) F. E. Hauser, C. D. Starr, L. Tietz and J. E. Dorn: Trans. ASM **47** (1955)

102–135.
18) D. Lahaie, J. D. Embury, M. M. Chadwick and G. T. Gray: Scr. Metall. Mater. **27** (1992) 139–142.
19) T. Mukai, M. Kawazoe and K. Higashi: Nano Structured Mater. **10** (1998) 755–765.
20) J. A. Chapman and D. V. Wilson: J. Inst. Metals **91** (1962–63) 39–40.
21) T. Mohri, M. Mabuchi, N. Saito and M. Nakamura: Mater. Sci. Eng. **A257** (1998) 287–294.
22) H. Yoshinaga and R. Horiuchi: Trans. JIM **5** (1963) 14–21.
23) A. Couret and D. Caillard: Acta Metall. **33** (1985) 1447–1454.
24) R. W. Armstrong: Metall. Trans. **1** (1970) 1169–1176.
25) C. J. Ball: J. Iron Stell. Inst. **191** (1959) 232–236.
26) A. Roy, U. Erb and H. Gleiter: Acta Metall. **30** (1982) 1847–1850.
27) T. Watanabe: Mater. Sci. Eng. **A176** (1994) 39–49.
28) T. Watanabe, S. Kimura and S. Karashima: Philos. Mag. **A 49** (1984) 845–864.
29) R. Z. Valiev, F. Chmelik, F. Bordeaux, G. Kapelski and B. Baudelet: Scr. Metall. Mater. **27** (1992) 855–860.
30) M. Furukawa, Z. Horita, M. Nemoto, R. Z. Valiev and T. G. Langdon: Acta Mater. **44** (1996) 4619–4629.
31) R. Z. Valiev, N. A. Krasilnikov and N. K. Tsenev: Mater. Sci. Eng. **A137** (1991) 35–40.
32) J. W. Wyrzykowski and M. W. Grabshi: Philos. Mag. **A 53** (1986) 505–520.
33) R. Z. Valiev, V. Yu. Gertsman and O. A. Kaibyshev: Phys. Status Solidi. (a) **97** (1986) 11.
34) A. A. Nazarov, A. E. Romanov and R. Z. Valiev: Acta Metall. Mater. **41** (1993) 1033–1040.